

Heteroatom-Induced Molecular Asymmetry Tunes Quantum Interference in Charge Transport through Single-Molecule Junctions

Yang Yang, Markus Gantenbein, Afaf Alqorashi, Junying Wei, Sara Sangtarash, Duan Hu, Hatef Sadeghi, Rui Zhang, Jiuchan Pi, Li-Chuan Chen, Xiaoyan Huang, Ruihao Li, Junyang Liu, Jia Shi, Wenjing Hong, Colin J. Lambert, and Martin R. Bryce

J. Phys. Chem. C, **Just Accepted Manuscript** • DOI: 10.1021/acs.jpcc.8b03023 • Publication Date (Web): 05 Jun 2018

Downloaded from <http://pubs.acs.org> on June 12, 2018

Just Accepted

“Just Accepted” manuscripts have been peer-reviewed and accepted for publication. They are posted online prior to technical editing, formatting for publication and author proofing. The American Chemical Society provides “Just Accepted” as a service to the research community to expedite the dissemination of scientific material as soon as possible after acceptance. “Just Accepted” manuscripts appear in full in PDF format accompanied by an HTML abstract. “Just Accepted” manuscripts have been fully peer reviewed, but should not be considered the official version of record. They are citable by the Digital Object Identifier (DOI®). “Just Accepted” is an optional service offered to authors. Therefore, the “Just Accepted” Web site may not include all articles that will be published in the journal. After a manuscript is technically edited and formatted, it will be removed from the “Just Accepted” Web site and published as an ASAP article. Note that technical editing may introduce minor changes to the manuscript text and/or graphics which could affect content, and all legal disclaimers and ethical guidelines that apply to the journal pertain. ACS cannot be held responsible for errors or consequences arising from the use of information contained in these “Just Accepted” manuscripts.



Heteroatom-Induced Molecular Asymmetry Tunes Quantum Interference in Charge Transport through Single-Molecule Junctions

*Yang Yang^{1#}, Markus Gantenbein^{2#}, Afaf Alqorashi^{3#}, Junying Wei¹, Sara Sangtarash³, Duan Hu¹, Hatef Sadeghi³, Rui Zhang¹, Jiuchan Pi¹, Lichuan Chen¹, Xiaoyan Huang¹, Ruihao Li¹, Junyang Liu¹, Jia Shi¹, Wenjing Hong^{*1}, Colin J. Lambert^{*3}, Martin R. Bryce^{*2}*

1. State Key Laboratory of Physical Chemistry of Solid Surfaces, Pen-Tung Sah Institute of Micro-Nano Science and Technology, College of Chemistry and Chemical Engineering, iChEM, Xiamen University, 361005, Xiamen, China

2. Department of Chemistry, Durham University, DH1 3LE, Durham, UK

3. Department of Physics, Lancaster University, LA1 4YB, Lancaster, UK

This manuscript is dedicated to the memory of Professor Thomas Wandlowski.

AUTHOR INFORMATION

Corresponding Author

* Wenjing Hong, Email: whong@xmu.edu.cn

* Martin R. Bryce, Email: m.r.bryce@durham.ac.uk

* Colin J. Lambert, Email: c.lambert@lancaster.ac.uk

ABSTRACT

We studied the interplay between quantum interference (QI) and molecular asymmetry in charge transport through a single molecule. Eight compounds with five-membered core rings were synthesized and their single-molecule conductances were characterized using the mechanically controllable break junction (MCBJ) technique. It is found that the symmetric molecules are more conductive than their asymmetric isomers and there is no statistically-significant dependence on the aromaticity of the core. In contrast, we find experimental evidence of destructive QI in five-membered rings, which can be tuned by implanting different heteroatoms into the core ring. Our findings are rationalized by the presence of anti-resonance features in the transmission curves calculated using non-equilibrium Green's functions. This novel mechanism for modulating QI effects in charge transport via tuning of molecular asymmetry will lead to promising applications in the design of single-molecule devices.

1. INTRODUCTION

Quantum interference (QI) effects have recently attracted great interest in studies of the charge transport at the single-molecule scale.¹⁻⁶ As determined by the phases of the partial de Broglie waves traversing different paths,⁷⁻⁹ QI provides a unique way to tune the single-molecule conductance by orders of magnitude without incorporating substituent groups, extending molecular length or changing the surrounding environment of the molecule. To date most reports of QI in cyclic molecules have been restricted to compounds with central six-membered rings.¹⁰⁻

¹⁴ Although it has not been observed experimentally, QI in central five-membered rings is

suggested to be a promising way to vary the molecular topology and increase structural diversity of single-molecule devices.¹⁵

The incorporation of heteroatoms into a central difunctionalized five-membered π -system leads to the structural asymmetry of the molecular junctions. Parks et al demonstrated that through modification of the symmetry of a single-molecule junction by axially stretching the molecule, the spin states, magnetic anisotropy, and thus the electron flow through the junction can be tuned.¹⁶ Our recent studies also suggest that an asymmetric pyridine (2,4-disubstituted) modifies the pattern of QI within the core of the molecular backbone and promotes charge transport through single-molecule junctions.¹⁷ Therefore, five-membered heterocyclic cores provide a logical diversification of the known structural platforms and enable an investigation of the interplay of QI effects and structural asymmetry of the core unit in charge transport through single-molecule junctions.

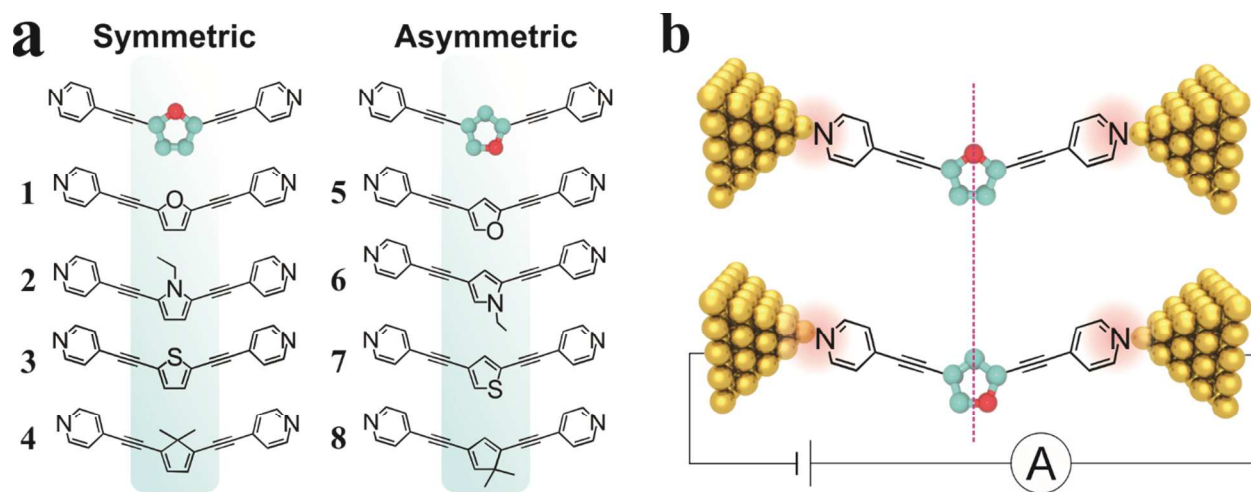


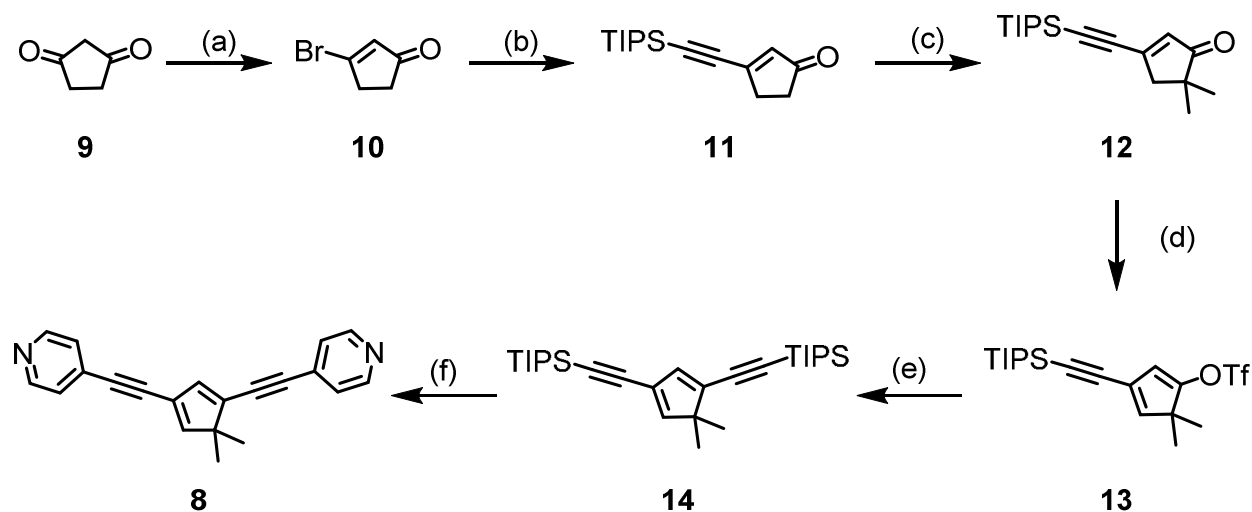
Figure 1. (a) Molecules with five-membered core units studied in this work. (b) Schematic of a molecular junction. The vertical dashed line shows the symmetry (top structure) and asymmetry (bottom structure) with respect to the core unit.

1
2
3 Herein we study the single-molecule conductances of a series of eight compounds of the type
4 X-Y-X. As shown in Figure 1a and Figures S3-1 and S3-2 in the SI, the furan (**1**, **5**), pyrrole (**2**,
5 **6**), thiophene (**3**, **7**) and cyclopentadiene cores (**4**, **8**) are rigid and planar. There are three notable
6 features in their molecular design: (i) all of the molecules have terminal pyridyl anchoring units
7 (X) at both ends; (ii) each molecule has one of four different five-membered core units (Y), and
8 (iii) the core is either symmetrically substituted (i.e. 2,5-difunctionalized; **1-4**) or asymmetrically
9 substituted (i.e. 2,4-difunctionalized; **5-8**). These compounds provide a unique opportunity to
10 investigate two issues. First, whether the QI effect is general for other conjugated systems,
11 besides those previously studied with aromatic six-membered central rings.¹⁰⁻¹⁴ Second, what is
12 the interplay between QI and structural asymmetry in charge transport through five-membered
13 core units?
14
15
16
17
18
19
20
21
22
23
24
25
26
27
28
29
30

31 2. EXPERIMENTAL SECTION

32
33 The synthesis and detailed characterization of compounds **1-8** are given in the SI. The general
34 synthetic strategy to the symmetrical target structures **1-4** was as follows. The core-unit 2,5-
35 disubstituted with bromine (thiophene, pyrrole, and furan) or triflate (cyclopentadiene) was
36 reacted with two equivalents of TIPS-protected acetylene under Sonogashira conditions. After a
37 two-pot reaction sequence of desilylation with tetrabutylammonium fluoride and subsequent
38 Sonogashira coupling with 4-iodopyridine, compounds **1-4** were obtained in good yields. The
39 synthesis of the asymmetric isomers **5-8** was more challenging. This was especially the case for
40 derivative **8** (Scheme 1) as the formation of C-C bonds at the 2,4-positions of cyclopentadiene
41 under mild conditions, to our knowledge is not known in the literature. It is worth noting that the
42
43
44
45
46
47
48
49
50
51
52
53
54
55
56
57
58
59
60

alkyne units at C(2) and C(4) were attached sequentially: this strategy should, therefore, be versatile for the attachment of different functionality at these positions.



Scheme 1. Synthesis of **8**. Reagents and Conditions: (a) PPh_3 , Br_2 , TEA, CH_2Cl_2 , $0\text{ }^\circ\text{C}$ to rt, 2 h, 71%; (b) $\text{PdCl}_2(\text{PPh}_3)_2$, CuI, TIPSA, DIPA, 10 min, 94%; (c) LiHMDS, MeI, THF, $-78\text{ }^\circ\text{C}$ to rt, 12 h, 64%; (d) KHMDS, Comins' reagent, THF, $-78\text{ }^\circ\text{C}$ to rt, 12 h, 87%; (e) TIPSA, $\text{PdCl}_2(\text{PPh}_3)_2$, CuI, TEA, THF, rt, 4 h, 91%; (f) TBAF (1 M in THF), THF, rt, 30 min, then 4-iodopyridine, $\text{PdCl}_2(\text{PPh}_3)_2$, CuI, THF, DIPA, $40\text{ }^\circ\text{C}$, 12 h, 61% (over two steps).

The mechanically controllable break junction (MCBJ) technique was used to measure the single-molecule conductances of compounds **1-8**. A schematic drawing of the molecular junction is shown in Figure 1b, while details of the electrical characterization are reported in our previous paper.¹⁸ Briefly, we use an Au wire tip of 99.99% purity for the in-situ fabrication of nanometer-sized separation. The target compounds were pre-pared as 0.2 mM solutions in TMB (mesitylene) as solvent. The experiments were carried out in ambient conditions at room

1
2
3 temperature by employing a homebuilt I - V converter with a sampling rate of 10 kHz. For each
4
5 conductance histogram, at least 1,000 individual curves were collected without any data
6
7 selection.
8
9

10 11 12 **3. RESULTS AND DISCUSSION** 13

14
15 Figures 2a and 2c display individual conductance traces of **1-4** and **5-8** recorded during the
16
17 opening process of the MCBJ operation. The corresponding conductance histograms are given in
18
19 Figures 2b and Figure 2d, respectively. Figures 2a-f are plotted in a semi-logarithmic scale in
20
21 order to cover the whole measuring range, and the conductance values are reported in units of the
22
23 conductance quantum ($G_0=2e^2/h$). As shown in Figure 2a, after an abrupt jump from the sudden
24
25 rupture of the last gold-gold atomic contact, clear conductance plateaus were observed which
26
27 could be attributed to the single molecular junctions.
28
29
30
31
32
33
34
35
36
37
38
39
40
41
42
43
44
45
46
47
48
49
50
51
52
53
54
55
56
57
58
59
60

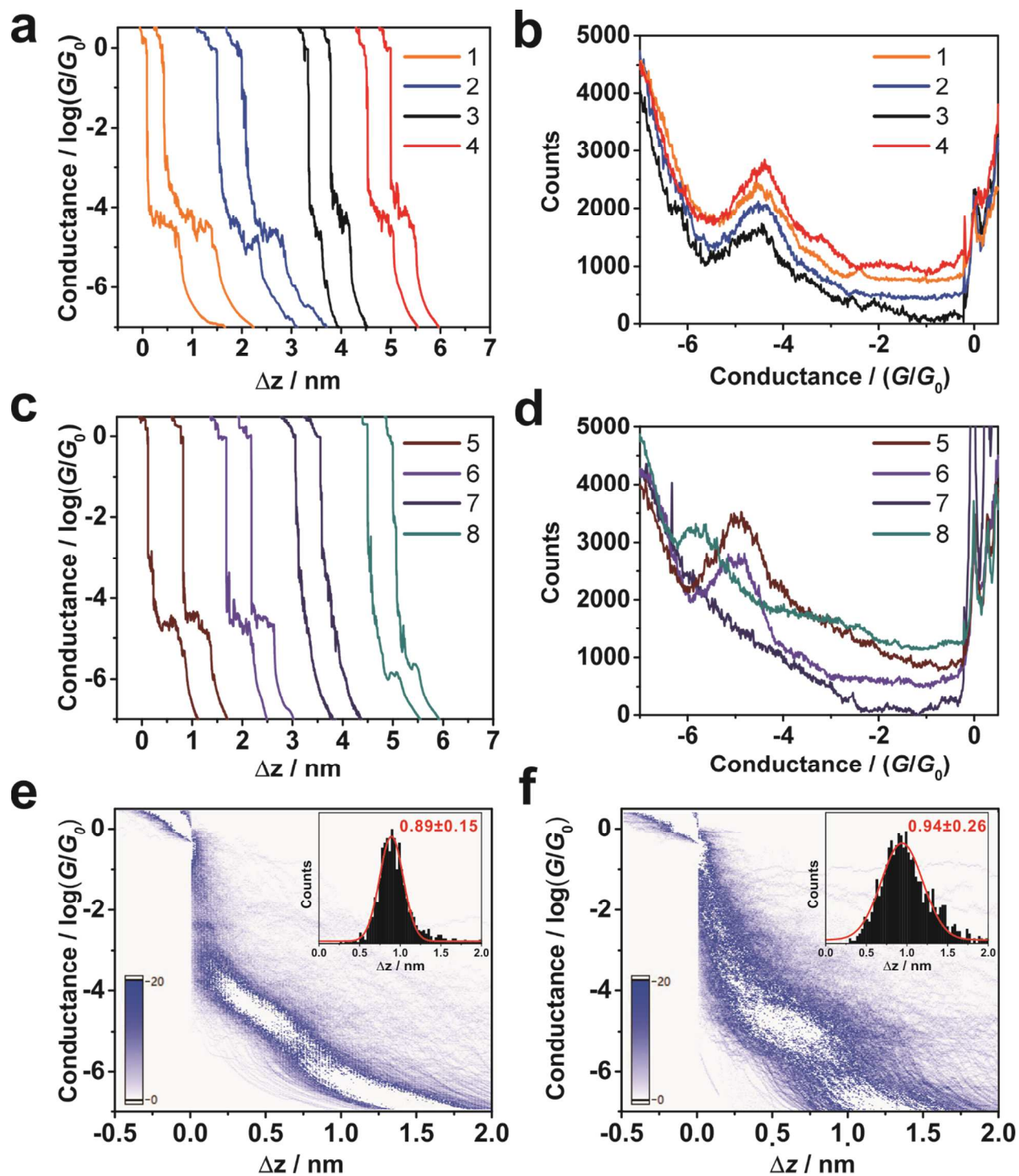


Figure 2. Typical conductance traces for compounds 1-4 (a) and 5-8 (c), respectively. One-dimensional conductance histograms for compounds 1-4 (b) and 5-8 (d), respectively. Two-

dimensional conductance-distance clouds of compounds **1** (e) and **5** (f), respectively. The curves in (b) and (d) are shifted for clarity, while the original histograms are given in the SI.

Table 1. Single-molecule conductances and lengths measured in MCBJ measurements.

Compounds	Measured Conductance / $\log(G/G_0)^a$	Measured Length / nm
1	-4.54 ± 0.37	1.39 ± 0.15
2	-4.57 ± 0.54	1.38 ± 0.18
3	-4.63 ± 0.36	1.36 ± 0.16
4	-4.49 ± 0.60	1.38 ± 0.13
5	-4.94 ± 0.40	1.44 ± 0.26
6	-5.03 ± 0.35	1.47 ± 0.23
7	$< -6^b$	/
8	-5.85 ± 0.34	1.40 ± 0.16

^a Error bars are based on the Gaussian fitting of conductance all-data-point one-dimensional histograms. The conductance of the symmetric isomers **1-4** divided by the conductance of the corresponding asymmetrical isomers **5-8**, respectively, gives the following values: **1/5** = 2.5; **2/6** = 2.9; **3/7** = >23.4; **4/8** = 22.9. ^b This is an assumed value, not a measured value. As discussed in the text, we conclude that the conductance of molecule **7** is below the instrumental sensitivity of our *I-V* converter, i.e., $< 10^{-6} G_0$.

The emergence of conductance plateaus in Figure 2a results in the discernible peaks in Figure 2b, which are centered at the very similar values of $10^{-4.54 \pm 0.37} G_0$, $10^{-4.57 \pm 0.54} G_0$, $10^{-4.63 \pm 0.36} G_0$, and $10^{-4.49 \pm 0.60} G_0$ for compounds **1-4**, respectively. The plateaus and peaks are attributed to the most favorable microscopic configuration of the molecular junctions, which were further verified by the location of the intensive cloud in the corresponding two-dimensional conductance-distance histograms, as shown in Figures 2e and 2f for compounds **1** and **5**. The comparable data for the other compounds and pure solvent are given in the SI. Based on the above-mentioned data analysis, Table 1 summarizes the single-molecule conductances and the lengths of

1
2
3 compounds **1-8** obtained from MCBJ measurements, where the length was calibrated by adding
4 0.5 nm considering the snap-back effect.¹⁸ In Table 1, error bars are based on the Gaussian fitting
5 of the one-dimensional conductance histograms and the plateau displacement distributions. For
6 compound **7** there is no distinct plateau in the individual trace, or peak in the conductance
7 histogram, implying that the single-molecule conductance is out of the measuring range of our *I*-
8 *V* converter, i.e., it is lower than $10^{-6} G_0$. We emphasize that we repeatedly attempted to measure
9 the conductance of molecule **7** with the same result on each occasion. In these experiments, all
10 the aspects of the instrumentation were checked, such as the notched-wire chip, the mechanical
11 components, as well as the *I-V* converter. Compound **7** is stable to storage under ambient
12 laboratory conditions, so decomposition of the molecules cannot explain this unexpected result.
13 We cannot prove that molecule **7** is binding in the junction, but there is no logical reason why it
14 should not bind, given that all the other seven molecules clearly do bind and reproducibly give
15 measurable conductance data.
16
17
18
19
20
21
22
23
24
25
26
27
28
29
30
31
32

33 The data show that for the symmetric compounds **1-4** there is no statistical variation of
34 conductance with the bridging atom (S, N, O or C). It is instructive to compare these results with
35 the work of Chen et al on a series of compounds having similar structures to **1**, **3**, and **4**.¹⁹ The
36 only difference is that each compound studied by Chen et al was wired to gold electrodes by
37 aminophenyl anchors, while the compounds studied here are wired by pyridyl anchors. The
38 molecular lengths in both studies are similar. Amino anchors lead to HOMO-dominated
39 conductances,²⁰ while pyridyl anchors lead to LUMO-dominated conductances,²¹ respectively.
40 For the amino anchors the clear trend in conductance was cyclopentadiene > furan > thiophene.
41 This led Chen et al to conclude that “aromaticity decreases single-molecule junction
42 conductance”.¹⁹ However, we conclude that for the symmetrical compounds **1-4** the pyridyl
43
44
45
46
47
48
49
50
51
52
53
54
55
56
57
58
59
60

1
2
3 anchor dominates the conductance, and there is no statistically-significant dependence on the
4 aromaticity of the core. Transport between the electrodes can occur through a continuous
5 linearly-conjugated “butadiene-type” pathway involving the four sp^2 -hybridized carbon atoms in
6
7
8 **1-4**. We also note that the single-molecule conductances of our pyridyl compounds are
9
10
11
12 consistently lower than for the amino anchored analogs due to the different anchoring groups.²²
13

14
15 Compounds **5-8** have isomeric structures and comparable lengths with **1-4**. However, the
16
17 single-molecule conductance values of **5-8** are consistently lower than that of the series **1-4** as
18
19 listed in Table 1, giving the direct evidence of destructive QI. This is logical based on a simple
20
21 resonance structure analysis of the cores disubstituted at the 2,4 positions,²³ suggesting the QI
22
23 rule in the conventional six-membered rings is also valid for five-membered rings. In contrast to
24
25 **1-4**, there is only weak effective coupling through the system in **5-8** as these molecules do not
26
27 offer a linearly conjugated pathway between the two leads. Connecting the substituents at the
28
29 2,4-positions of the core (compounds **5-8**) corresponds to cross-conjugation,^{4,24} thus resulting in
30
31 destructive QI. This finding is reminiscent of data for six-membered phenyl core units, where
32
33 destructive QI has been observed in the case of non-conjugated *meta* couplings,¹⁰⁻¹⁴ and of our
34
35 recent work with polycyclic core units, which established that the resonance energy of the core
36
37 influences single-molecule conductance.²⁵ In the present case, there is no effective conjugated
38
39 pathway in molecules **5-8**, therefore, the heteroatom in **5-7**, or the sp^3 carbon atom in **8**, plays a
40
41 more important role in determining the conductance than in series **1-4**.
42
43
44
45

46
47 For compounds **5-8**, the electronegativity decreases in the sequence O (3.44) > N (3.04) > S
48
49 (2.58) \approx C (2.55) from the periodic table of electronegativity by the Pauling scale, thus for the
50
51 studied compounds, the degree of asymmetry decreases in the sequence **5** > **6** > **7** \approx **8**. The
52
53 degrees of asymmetry are tuned by the electronegativity of the heteroatom in **5-7**, or the sp^3
54
55
56
57
58
59
60

carbon atom in **8**. As listed in Table 1, the lowest conductance values are obtained for **7** and **8**, where the heteroatoms have the lowest electronegativities, suggesting a strong correlation between the molecular asymmetry, electronegativity and single-molecule conductance.

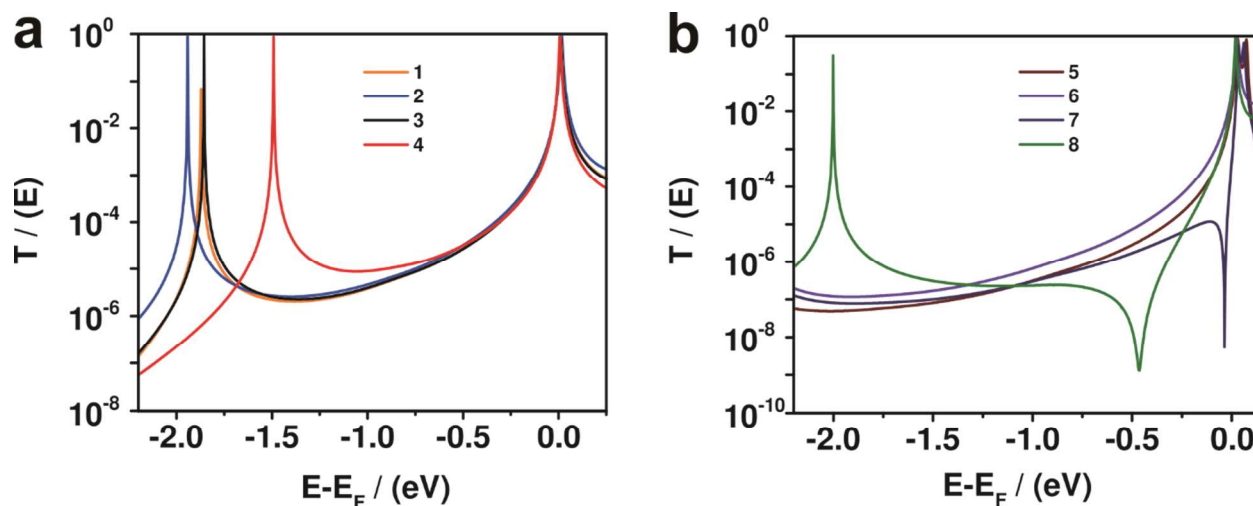


Figure 3. DFT results of the transmission coefficients for (a) compounds **1-4** and (b) **5-8**.

To investigate the interplay between structural asymmetry and QI in molecules wired between two electrodes, we calculated the transmission coefficient $T(E)$ of electrons with energy E passing from one electrode to another through molecules shown in Figure S3-2, using the Gollum transport code.²⁶ Figure 3 shows the calculated $T(E)$ of compounds **1-8** using the material specific mean field Hamiltonian obtained from the SIESTA implementation of density functional theory (DFT).²⁷ For molecules with pyridyl terminal groups, it is known that DFT incorrectly places the Fermi energy close to the LUMO resonance (at $E-E_F = 0$ in Figure 3). This causes DFT to overestimate the conductance and therefore to achieve agreement with experiment, the Fermi energy should be shifted away from the LUMO towards the middle of the HOMO-LUMO gap (near $E-E_F = -1$ eV in Figure 3).²¹ Such a shift is consistent with

1
2
3 thermopower measurements of pyridyl-terminated molecules, whose positive Seebeck
4 coefficients indicate that the Fermi energy lies in the tail of the LUMO, (in the range $-1 \text{ eV} < E-$
5 $E_F < 0$ in Figure 3).²⁸ For the symmetric compounds, Figure 3 shows that the $T(E)$ values of **1-4**
6
7
8 in the LUMO dominated regime $-1 \text{ eV} < E < 0$ are quite similar, in good agreement with the
9
10 experimental findings, that for the series **1-4** the conductances are almost the same. Nevertheless,
11
12 in other cases the conductances of *para* compounds with pyridyl may be sensitive to the
13
14 heteroatoms. For instance, recently we measured the conductances of a series of *para*
15
16 compounds with polycyclic core units, i.e., dibenzothiophene, carbazole, dibenzofuran and
17
18 fluorene cores, where the conductance varies as the heteroatom changes because the transmission
19
20 around the LUMO peak is sensitive to the heteroatoms.²⁵
21
22
23
24
25

26 As shown in Figure 3b, in the same energy regime $-1 \text{ eV} < E < 0$, the calculated $T(E)$ of **5-8** is
27
28 significantly lower than that of **1-4**. Furthermore, for compounds **7** and **8**, sharp drops in the
29
30 transmission curve, i.e., the anti-resonance features, are observed in the tail of the LUMO peaks.
31
32 The presence of these anti-resonances correlates with the lower measured conductances for these
33
34 compounds. In contrast, for **5** and **6**, as shown in Figure 3b, there are no anti-resonances within
35
36 the HOMO-LUMO gap, which correlates with the higher conductances that are measured
37
38 experimentally. The absence of anti-resonance features within the HOMO-LUMO gap suggests
39
40 that the high electronic asymmetry of the core unit, which originates from the greater
41
42 electronegativities of the heteroatoms, moves the anti-resonance features out of the HOMO-
43
44 LUMO gap of the molecular junction, and thus QI has a minor effect on the charge transport
45
46 through single-molecule junctions. These theoretical results and our experimental findings
47
48 suggest that molecular asymmetry affords a novel approach to tuning destructive QI and charge
49
50 transport through single-molecule junctions.
51
52
53
54
55
56
57
58
59
60

4. CONCLUSIONS

To conclude, we investigated the synergistic effect of molecular symmetry and QI on the charge transport through single-molecule junctions with five-membered core rings. The study of 5-membered ring cores is a new and promising way to increase structural diversity of single-molecule devices. It was found that for the symmetric 2,5-disubstituted series **1-4**, the pyridyl anchors dominate the conductance and there is no statistically significant variation with core unit. In contrast, the conductances of the asymmetric 2,4-disubstituted series **5-8** are significantly lower than those of the symmetric **1-4** series, reflecting the presence of destructive QI. More importantly, the control of molecular asymmetry via the heteroatoms provides the tuning of destructive QI in the charge transport through single-molecule junctions. DFT calculations reveal that for asymmetric molecules, the electronegativity of the heteroatoms can be used to move anti-resonance features into or out of the HOMO-LUMO gap, which controls the destructive QI effect. Our work establishes a route for the design of building blocks through incorporating heteroatoms into molecular structure, and further demonstrates a novel yet simple strategy for tuning QI in single-molecule electronics via asymmetry. This has promising applications in the design of future molecular-electronic components

AUTHOR INFORMATION

Corresponding Author

* Wenjing Hong, Email: whong@xmu.edu.cn

* Colin J. Lambert, Email: c.lambert@lancaster.ac.uk

* Martin R. Bryce, Email: m.r.bryce@durham.ac.uk

Author Contributions

#Yang Yang, Markus Gantenbein and Afaf Alqorashi contributed equally to this work.

Notes

The authors declare no competing financial interests.

SUPPORTING INFORMATION

The Supporting Information is available free of charge on the ACS Publications website at DOI: Synthesis and characterization of compounds **1-8**; methods and results for the single-molecule conductance measurements of solvent and compounds **1-8**; computational methods for calculating the transmission coefficients.

ACKNOWLEDGMENTS

We thank the National Natural Science Foundation of China (21503179, 21673195, 21722305, 21703188), the Natural Science Foundation of Fujian Province (2016J05162), the National Key R&D Program of China (2017YFA0204902), the Fundamental Research Funds for the Central Universities (Xiamen University: 20720170035) and Young Thousand Talent Project for funding work in Xiamen; EC FP7 ITN ‘MOLESCO’ project number 606728 for funding work in Durham and Lancaster; UK EPSRC grant EP/K0394/23/1 for funding instrumentation used in Durham and grants EP/N017188/1, EP/M014452/1 in Lancaster.

REFERENCES

- (1) Baer, R.; Neuhauser, D. Phase Coherent Electronics: A Molecular Switch Based on Quantum Interference. *J. Am. Chem. Soc.* **2002**, *124*, 4200-4201.
- (2) Cardamone, D. M.; Stafford, C. A.; Mazumdar, S. Controlling Quantum Transport through a Single Molecule. *Nano Lett.* **2006**, *6*, 2422-2426.

1
2
3 (3) Guedon, C. M.; Valkenier, H.; Markussen, T.; Thygesen, K. S.; Hummelen, J. C.; van der
4 Molen, S. J. Observation of Quantum Interference in Molecular Charge Transport. *Nat.*
5 *Nanotechnol.* **2012**, *7*, 305-309.

6
7
8 (4) Valkenier, H.; Guedon, C. M.; Markussen, T.; Thygesen, K. S.; van der Molen, S. J.;
9 Hummelen, J. C. Cross-Conjugation and Quantum Interference: A General Correlation? *Phys.*
10 *Chem. Chem. Phys.* **2014**, *16*, 653-662.

11
12 (5) Lambert, C. J. Basic Concepts of Quantum Interference and Electron Transport in Single-
13 Molecule Electronics. *Chem. Soc. Rev.* **2015**, *44*, 875-888.

14
15 (6) Su, T. A.; Neupane, M.; Steigerwald, M. L.; Venkataraman, L.; Nuckolls, C. Chemical
16 Principles of Single-Molecule Electronics. *Nat. Rev. Mater.* **2016**, *1*, No. 16002.

17
18 (7) Geng, Y.; Sangtarash, S.; Huang, C.; Sadeghi, H.; Fu, Y.; Hong, W.; Wandlowski, T.;
19 Decurtins, S.; Lambert, C. J.; Liu, S.-X. Magic Ratios for Connectivity-Driven Electrical
20 Conductance of Graphene-Like Molecules. *J. Am. Chem. Soc.* **2015**, *137*, 4469-4476.

21
22 (8) Sangtarash, S.; Huang, C. C.; Sadeghi, H.; Sorohhov, G.; Hauser, J.; Wandlowski, T.;
23 Hong, W. J.; Decurtins, S.; Liu, S. X.; Lambert, C. J. Searching the Hearts of Graphene-Like
24 Molecules for Simplicity, Sensitivity, and Logic. *J. Am. Chem. Soc.* **2015**, *137*, 11425-11431.

25
26 (9) Sangtarash, S.; Sadeghi, H.; Lambert, C. J. Exploring Quantum Interference in
27 Heteroatom-Substituted Graphene-Like Molecules. *Nanoscale* **2016**, *8*, 13199-13205.

28
29 (10) Solomon, G. C.; Herrmann, C.; Hansen, T.; Mujica, V.; Ratner, M. A. Exploring Local
30 Currents in Molecular Junctions. *Nat. Chem.* **2010**, *2*, 223-228.

31
32 (11) Arroyo, C. R.; Frisenda, R.; Moth-Poulsen, K.; Seldenthuis, J. S.; Bjornholm, T.; van der
33 Zant, H. S. J. Quantum Interference Effects at Room Temperature in Opv-Based Single-
34 Molecule Junctions. *Nanoscale Res. Lett.* **2013**, *8*, No. 234.

35
36 (12) Arroyo, C. R.; Tarkuc, S.; Frisenda, R.; Seldenthuis, J. S.; Woerde, C. H. M.; Eelkema,
37 R.; Grozema, F. C.; van der Zant, H. S. J. Signatures of Quantum Interference Effects on Charge
38 Transport through a Single Benzene Ring. *Angew. Chem. Int. Ed.* **2013**, *52*, 3152-3155.

39
40 (13) Manrique, D. Z.; Huang, C.; Baghernejad, M.; Zhao, X.; Al-Owaedi, O. A.; Sadeghi, H.;
41 Kaliginedi, V.; Hong, W.; Gulcur, M.; Wandlowski, T.; et al. A Quantum Circuit Rule for
42 Interference Effects in Single-Molecule Electrical Junctions. *Nat. Commun.* **2015**, *6*, No. 6389.

1
2
3 (14) Garner, M. H.; Solomon, G. C.; Strange, M. Tuning Conductance in Aromatic
4 Molecules: Constructive and Counteractive Substituent Effects. *J. Phys. Chem. C* **2016**, *120*,
5 9097-9103.
6
7

8 (15) Borges, A.; Solomon, G. C. Effects of Aromaticity and Connectivity on the Conductance
9 of Five-Membered Rings. *J. Phys. Chem. C* **2017**, *121*, 8272-8279.
10
11

12 (16) Parks, J. J.; Champagne, A. R.; Costi, T. A.; Shum, W. W.; Pasupathy, A. N.;
13 Neuscamman, E.; Flores-Torres, S.; Cornaglia, P. S.; Aligia, A. A.; Balseiro, C. A.; et al.
14 Mechanical Control of Spin States in Spin-1 Molecules and the Underscreened Kondo Effect.
15 *Science* **2010**, *328*, 1370-1373.
16
17

18 (17) Liu, X. S.; Sangtarash, S.; Reber, D.; Zhang, D.; Sadeghi, H.; Shi, J.; Xiao, Z. Y.; Hong,
19 W. J.; Lambert, C. J.; Liu, S. X. Gating of Quantum Interference in Molecular Junctions by
20 Heteroatom Substitution. *Angew. Chem. Int. Ed.* **2017**, *56*, 173-176.
21
22

23 (18) Hong, W.; Valkenier, H.; Meszaros, G.; Manrique, D. Z.; Mishchenko, A.; Putz, A.;
24 Garcia, P. M.; Lambert, C. J.; Hummelen, J. C.; Wandlowski, T. An Mcbj Case Study: The
25 Influence of Pi-Conjugation on the Single-Molecule Conductance at a Solid/Liquid Interface.
26 *Beilstein J. Nanotechnol.* **2011**, *2*, 699-713.
27
28

29 (19) Chen, W.; Li, H.; Widawsky, J. R.; Appayee, C.; Venkataraman, L.; Breslow, R.
30 Aromaticity Decreases Single-Molecule Junction Conductance. *J. Am. Chem. Soc.* **2014**, *136*,
31 918-920.
32
33

34 (20) Dell'Angela, M.; Kladnik, G.; Cossaro, A.; Verdini, A.; Kamenetska, M.; Tamblyn, I.;
35 Quek, S. Y.; Neaton, J. B.; Cvetko, D.; Morgante, A.; et al. Relating Energy Level Alignment
36 and Amine-Linked Single Molecule Junction Conductance. *Nano Lett.* **2010**, *10*, 2470-2474.
37
38

39 (21) Bagrets, A.; Arnold, A.; Evers, F. Conduction Properties of Bipyridinium-Functionalized
40 Molecular Wires. *J. Am. Chem. Soc.* **2008**, *130*, 9013-9018.
41
42

43 (22) Hong, W.; Manrique, D. Z.; Moreno-Garcia, P.; Gulcur, M.; Mishchenko, A.; Lambert,
44 C. J.; Bryce, M. R.; Wandlowski, T. Single Molecular Conductance of Tolanes: Experimental
45 and Theoretical Study on the Junction Evolution Dependent on the Anchoring Group. *J. Am.*
46 *Chem. Soc.* **2012**, *134*, 2292-2304.
47
48

49 (23) Markussen, T.; Stadler, R.; Thygesen, K. S. The Relation between Structure and
50 Quantum Interference in Single Molecule Junctions. *Nano Lett.* **2010**, *10*, 4260-4265.
51
52
53
54
55
56
57
58
59
60

1
2
3 (24) Pedersen, K. G. L.; Borges, A.; Hedegard, P.; Solomon, G. C.; Strange, M. Illusory
4 Connection between Cross-Conjugation and Quantum Interference. *J. Phys. Chem. C* **2015**, *119*,
5 26919-26924.
6
7

8 (25) Gantenbein, M.; Wang, L.; Al-Jobory, A. A.; Ismael, A. K.; Lambert, C. J.; Hong, W. J.;
9 Bryce, M. R. Quantum Interference and Heteroaromaticity of Para- and Meta-Linked Bridged
10 Biphenyl Units in Single Molecular Conductance Measurements. *Sci. Rep.* **2017**, *7*, No. 1794.
11
12

13 (26) Ferrer, J.; Lambert, C. J.; García-Suárez, V. M.; Manrique, D. Z.; Visontai, D.;
14 Oroszlany, L.; Rodríguez-Ferradás, R.; Grace, I.; Bailey, S. W. D.; Gillemot, K.; et al. Gollum:
15 A Next-Generation Simulation Tool for Electron, Thermal and Spin Transport. *New J. Phys.*
16 **2014**, *16*, No. 093029.
17
18
19

20 (27) José, M. S.; Emilio, A.; Julian, D. G.; Alberto, G.; Javier, J.; Pablo, O.; Daniel, S.-P. The
21 Siesta Method for Ab Initio Order- N Materials Simulation. *J. Phys-Condens. Mat.* **2002**, *14*,
22 2745-2779.
23
24

25 (28) Rincon-Garcia, L.; Evangeli, C.; Rubio-Bollinger, G.; Agrait, N. Thermopower
26 Measurements in Molecular Junctions. *Chem. Soc. Rev.* **2016**, *45*, 4285-4306.
27
28
29
30
31
32
33
34
35
36
37
38
39
40
41
42
43
44
45
46
47
48
49
50
51
52
53
54
55
56
57
58
59
60

TOC Graphic

